中国激光

基于拉曼光谱技术的精子评筛研究进展

黄祖芳[1*]，李玉玲[1]，杜生荣[2]，孙艳[2]，王佳睿[1]，张群[1]，陈荣[1]

[1]福建师范大学光电与信息工程学院，医学光电科学与技术教育部重点实验室，福建省光子技术重点实验室，福建 福州 350117；
[2]福建省妇幼保健院辅助生殖中心，福建 福州 350001

摘要 全球成年男性的精子质量呈明显下降趋势。精子质量下降与男性不育虽并非线性关系，但显然与低生育力密切相关。辅助生殖技术针对不育男性精子水平低、形态和运动活力异常等常见问题，通过评估和筛选优质精子，提供了解决男性不育问题的主要技术方案。现有临床研究局限于精子形貌和活力等特征参数的筛选，缺乏针对精子DNA损伤情况的无损评筛手段。本文首先介绍了精子无损评筛技术在辅助生殖领域男科的应用需求以及显微拉曼光谱技术的基本原理，继而对基于拉曼光谱技术的精子研究进行了综述，综合分析探讨了精子的拉曼光谱检测和光谱特征，聚焦精子DNA损伤的拉曼光谱响应问题，最后讨论和展望了精子无损评筛技术的发展前景。

关键词 医用光学；拉曼光谱；精子；DNA损伤；评估筛选；统计分析

中图分类号 Q492 **文献标志码** A **DOI**：10.3788/CJL230472

1 引 言

最新统计表明，全球约10%～15%的夫妇存在不同程度的生育障碍，中国已婚人群中不孕不育比例达7%～10%，不孕不育患者人数呈逐年快速上升趋势[1]。不孕不育问题已成为继肿瘤和心血管疾病之后的重大全球性健康问题，关乎人类的生存繁衍和可持续健康发展。男性因素导致的不育症接近不育症总体的50%[2]，主要表现为少精子症、弱精子症、畸形精子症、死精子症及无精子症等。

男性不育因素复杂，环境污染、不健康的生活方式、性传染病以及癌症等因素是导致男性不育的主因[3]。遗憾的是，目前针对男性不育的传统药物治疗手段存在治疗过程耗时、缺乏特异性效果等问题。若治疗不当，可造成终身不育，影响家庭和睦，危及社会稳定。辅助生殖技术（ART）是治疗不孕不育的重要手段，主要包括子宫内授精（IUI）[4]、体外受精（IVF）[5]和卵胞浆内单精子显微注射（ICSI）[6]。ICSI技术，俗称第二代“试管婴儿”，是借助显微镜筛选单个高质量精子并将其直接注射到卵细胞中实现精卵结合，从而形成受精的一种显微操作技术。该技术具有受精率高等优点，已成为男性严重少精子症、弱精子症、畸形精子症患者及不明原因的不育症患者极为重要的甚至是唯一有效的治疗方法[1,7-8]，为男性不育症的治疗带来了革命性突破。

ICSI技术将单个精子直接注入到卵母细胞内形成受精的操作，无疑规避了精卵结合的选择过程，精子未能经历女性生殖道的优胜劣汰筛选。ICSI技术的成功率取决于精子质量和显微操作技能，因而形态优良、具有受精潜能的生理活性精子评估筛选是ICSI成功的重要前提和关键。目前，临床上常规ICSI的精子筛选方法包括精子上游法和密度梯度离心法。前者利用精液中的精子上游到培养液上层的能力差异来实现优质精子与活动力差精子、死精子、细胞碎屑等的分离筛选[9]。密度梯度离心方法[10]则是根据密度梯度溶液柱中的正常精子与畸形精子、不活动精子及精液中的其他细胞成分在运动能力、运动轨迹和浮力密度等方面的差异，使离心后的精液中的各种成分在密度梯度溶液柱中达到平衡并停留在各自的等浮力密度点上，进而实现正常精子的分离。上述两种方法虽然可以筛选出形态和活动力俱佳的精子，但却无法实现DNA损伤精子的筛除。此外，直接上游法回收的精子量少（尤其是精子浓度非常低的精液样品），而密度梯度离心法易造成活性氧的产生，增大了精子DNA损伤的潜在风险[11]。

研究表明，不育或低生育能力男性患者精液中形态正常的精子在很大比例上存在不同程度的DNA损伤[12]，一旦这些形态看似完好但DNA有损的精子被筛选用于受精，无疑将直接影响后续胚胎发育的质量，导致不良的妊娠结局，甚至导致子代的出生缺陷[12]，更有甚者，受损DNA遗传到下一代，影响子代的健康和生育能力[13-14]。常见的精子DNA损伤评估方法，如精子

收稿日期：2023-02-01；**修回日期**：2023-03-10；**录用日期**：2023-04-01；**网络首发日期**：2023-04-14

基金项目：国家自然科学基金（62275049，11874006，82170908）、福建省自然科学基金重点项目（2022J02024）

通信作者：*zfhuang@fjnu.edu.cn

染色质结构分析试验(SCSA)[15]、彗星试验[16]、末端转移酶介导的dUTP末端标记法[17]、染色质扩散试验(SCD)[18]等,均需对精子进行染色处理,使得即便检测评估为正常的精子也因染色操作后无法用于与卵细胞形成受精。因而,针对活动精子的DNA质量(完整性)无损评估筛选不仅有助于提供真正的优质精子,更有望协助解决男性生育能力下降的问题。

光谱学是研究光与物质相互作用的学科。光谱仪借助光栅或棱镜将光分成不同波长的分量,输出光强度是波长的函数,通过测量光与物质的相互作用可从中获得检测对象的生化成分及含量信息。其中,振动光谱技术作为化合物结构表征和分析的重要工具,具有检测无损、高灵敏度等优点。随着光谱仪和检测技术的高速发展,该技术已被广泛应用于生物医学领域[19-20]。代表性的振动光谱技术——拉曼光谱检测技术,利用非弹性散射获得反映物质组成成分及物质分子结构的信息,被广泛应用于材料科学、生物医学科学等领域的检测和分析研究。此外,拉曼光谱技术具有其他检测技术所不具备或无法同时兼具的优点,如:测量不受水的干扰,样品无须制备或外源性标记,可无损、快速获得物质分子的"指纹"生化信息。显微拉曼光谱技术借助显微镜系统可以获得优异的横向空间分辨率,实现微米尺度感兴趣区域检测对象的拉曼光谱信号检测。显微拉曼光谱技术已在组织、细胞及生物分子的光谱检测及光谱成像中获得广泛应用[21-27]。近年来,基于拉曼光谱技术的体液研究备受关注,唾液、血液、尿液等体液的拉曼光谱研究取得了一定突破和进展[28-31]。相较于常规方法局限于精子形貌和活动力的评估和筛选,基于显微拉曼光谱技术的精子研究可客观地反映精子生化信息(尤其是DNA质量),凸显无损评估的独特优势。

本文总结了近年来基于拉曼光谱技术的精子研究进展,分析探讨了精子的拉曼光谱检测和光谱响应特征,聚焦精子DNA损伤的拉曼光谱响应研究等问题,对现有研究存在的不足进行了分析,并对优质精子评筛潜在的发展方向进行了展望。

2 显微拉曼光谱技术的基本原理

光波与物质相互作用时可被反射、吸收、透射或散射。其中,光与物质发生散射作用时,部分光发生最常见的弹性散射(散射光与入射光的波长相同),另外少部分光发生非弹性散射(即散射光具有比入射光更高或更低的频率),也称为拉曼散射。显然,这一非弹性散射过程会导致部分光子的能量发生改变,这种能量改变与物质分子的官能团、分子结构以及分子环境等直接相关。原理上,单一波长的光(通常为激光)聚焦到样品上,样品分子吸收光子后被激发到较高的、不稳定的虚能态,随后电子弛豫跃迁到振动能级并发光,其中部分光的波长红移或蓝移;频率小于入射光频率的谱线称为斯托克斯光线,而频率大于入射光频率的谱线称为反斯托克斯光线,如图1所示。

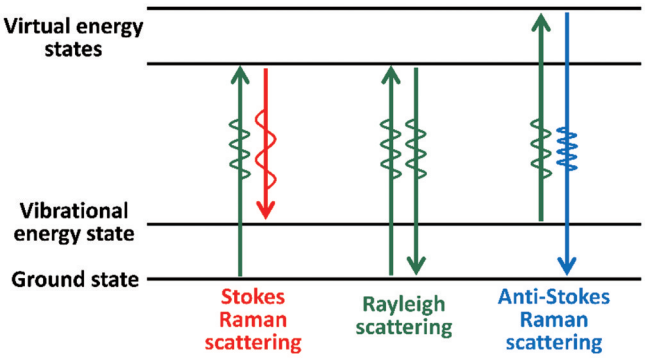

图1 拉曼散射能级示意图

Fig. 1 Energy level diagram for Raman scattering process

简言之,拉曼光谱技术是一种光的非弹性散射技术,基于光与物质分子化学键的相互作用来获得反映物质分子及其官能团振动模式的特征性光谱信息。一般而言,分子的对称性振动和非极性基团的振动可引发分子形变,导致分子的极化率随之变化,进而表现出拉曼活性。研究表明,生物分子均表现为拉曼活性分子。

不同于传统的拉曼光谱技术,显微拉曼光谱技术是结合了拉曼光谱和显微光学成像的技术。由专门设计的拉曼光谱仪和光学显微成像系统组成的显微拉曼光谱仪,允许操作人员开展宏观样品的微观区域观察以及对样品进行显微水平的拉曼光谱检测。相比于非显微检测模式,其所具有的显著优势在于:1) 显微拉曼检测仅需微量甚至痕量样品;2) 以"所见即所得"的方式获得感兴趣区域的拉曼光谱测量结果;3) 可在局部区域实现某些效果增强。

3 精子的显微拉曼光谱研究

在精子完整性的光学研究方面,最早Itzkan等[32]采用共聚焦光吸收和散射技术(CLASS)开展了正常和DNA受损精子细胞的研究。Gianaroli等[33]采用偏振光研究了精子头部的双折射现象,进而评估了精子顶体状态与ICSI结果的相关性。拉曼光谱技术在唾液、血液、尿液等体液研究中受到了极大重视并实现了快速发展[28-31],虽然其在精子研究方面尚处于初步发展阶段,但其所具有的独特优势无疑为精子研究开拓了新方向和新思路。

3.1 非活性精子的显微拉曼光谱研究

2009年,Huser等[34]采用显微拉曼光谱技术研究了单精子细胞中染色质差异的拉曼光谱响应与精子细胞形貌的相关性。精子细胞的显微拉曼光谱可用于评估精子细胞的DNA包装效率。虽然正常和异常形貌精子细胞的相对蛋白质含量与DNA包装效率存在一定的交叉性,但绝大部分正常形貌精子细胞的拉曼光

谱提示DNA的有效包装。随后，Meister等[35]基于共聚焦显微拉曼光谱系统，采用532 nm激发波长，实现了精子细胞核、颈部以及精子细胞中部线粒体的拉曼光谱成像刻画表征，如图2所示。

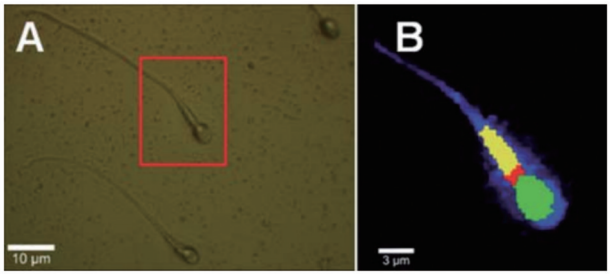

图2 精子细胞的明场光学图像(A)和拉曼光谱成像刻画(B)[35]

Fig. 2 Bright-field optical image of human sperm cells (A) and chemical mapping constructed from sperm Raman spectra (B)[35]

Meister等[35]通过模拟紫外线辐射对精子不同细胞器的损伤，并尝试量化拉曼光谱特征，验证了显微拉曼光谱法有望成为快速评估精子线粒体状态的新方法。鉴于精子的DNA损伤主要是由活性氧引起的，2011年，Mallidis等[36]采用紫外线照射的方式引发精子DNA损伤，并详细对比了精子样品的拉曼光谱响应差异，结果发现精子DNA损伤主要反映在归属于DNA的PO_4骨架峰(1042 cm^{-1})的强度变化上。此外，他们基于小波分解方法证实了1042 cm^{-1}谱峰及另一个UVB敏感区域(1400～1600 cm^{-1})对应于精子头部区域蛋白质-DNA的相互作用，如图3所示。da Costa等[37]对比了不同环境下受紫外线辐照与未受紫外线辐照的精子的拉曼光谱响应，结果显示：紫外线造成的精子DNA损伤光谱响应仅在干燥条件下能观察到，在溶液介质则观察不到。

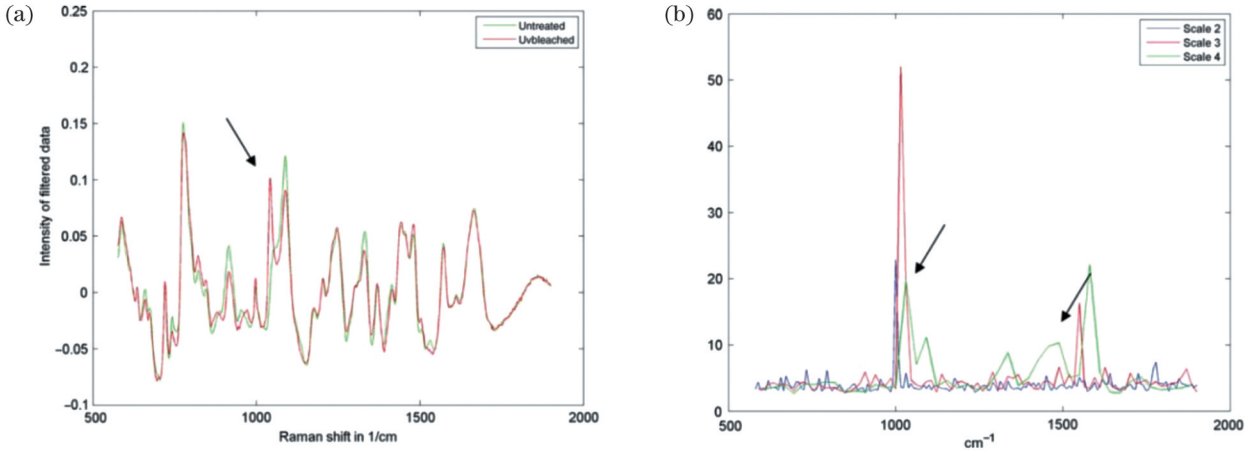

图3 平均光谱及小波系数分布[36]。(a)平均光谱，未受紫外线辐照的精子(绿色)与受UVB辐照(红色)的精子的光谱在1042 cm^{-1}(箭头)处有明显差异；(b)受UVB辐照的精子的小波系数分布

Fig. 3 Averaged spectra and wavelet coefficient distributions[36]. (a) Average spectra showing the distinct difference at 1042 cm^{-1} (arrow) in spectra of UVB irradiated (red) and untreated (green) sperms; (b) wavelet coefficient distribution of UVB irradiated sperm

为进一步优化和验证显微拉曼光谱识别氧化应激引起的精子DNA损伤的可靠性，2012年，德国明斯特大学生殖医学和男性医学中心研究小组[38]对比了精子的拉曼测试结果和流式细胞仪分析结果，发现不同程度DNA损伤的精子的拉曼光谱特征峰位强度存在响应差异，尤其是当归属于DNA磷酸骨架的1050 cm^{-1}和1095 cm^{-1}峰位强度的比值大于界限值0.63时，精子头部的氧化性DNA损伤比例与DNA碎片指数(DFI)呈线性关系，如图4所示。

虽然精子质量的拉曼刻画已获得认可，但先前的研究存在精子样品制备耗时等问题(如过夜干燥)，进而可能会对拉曼测试结果产生影响。为此，2013年，Huang等[39]基于新型拉曼测试基底采集正常和各种异常形貌(梨形、锥形、小头型)精子的显微拉曼光谱数据(如图5所示)，随后基于主成分分析和线性判别(PCA-LDA)方法进行分类。结果显示：该方法区分正常和异常形貌精子的诊断灵敏度为76%，特异性为91%，准确率为80%。该工作主要针对先前的精子拉曼光谱检测存在样品制备耗时的问题，实现了新型基底下精子细胞显微拉曼光谱检测样品的快速(十几秒)制备。

上述精子DNA完整性的显微拉曼光谱评估均对拉曼检测基底有一定要求(适合精子形态观察，无拉曼背景干扰等)，鉴于此，Du等[40]尝试在载玻片上对DNA完整和DNA受损精子细胞进行了拉曼光谱检测。他们采用扩展乘法信号校正(EMSC)方法有效“滤除”了玻璃基底信号的干扰，获得了玻璃基底上精子的本征拉曼信号。此外，针对目前精子拉曼光谱检测结果局限于一定数量精子的统计分析，缺乏单精子拉曼结果与真实染色评估的一一对应验证，他们基于玻璃基底上精子的染色分析，实现了基底上精子细胞DNA的拉曼光谱及DNA染色结果的严格一对一验证，结果如图6所示。

虽然DNA损伤精子和DNA完整精子细胞的拉曼

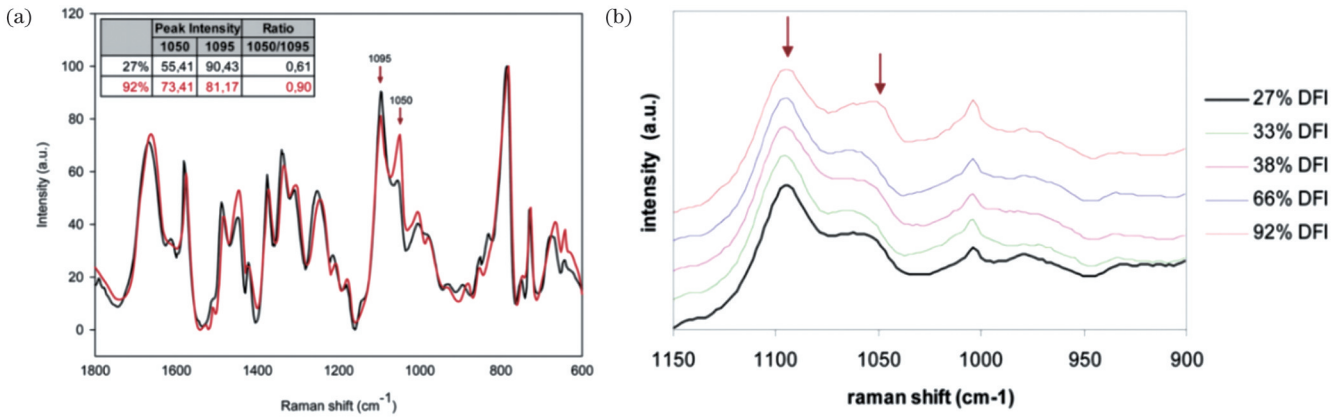

图 4 拉曼光谱[38]。(a)未处理精子(27% DFI,黑色)和诱导氧化性 nDNA 损伤精子(92% DFI,红色)的拉曼光谱比较;(b)DNA PO_4 骨架对应区域的拉曼光谱表明了不同程度的氧化损伤

Fig. 4 Raman spectra[38]. (a) Raman spectra comparison of untreated sperm (27% DFI, black) and the sperm induced with oxidative nDNA damage (92% DFI, red); (b) Raman spectra in the region corresponding to the DNA PO_4 backbone indicating different levels of oxidative damage

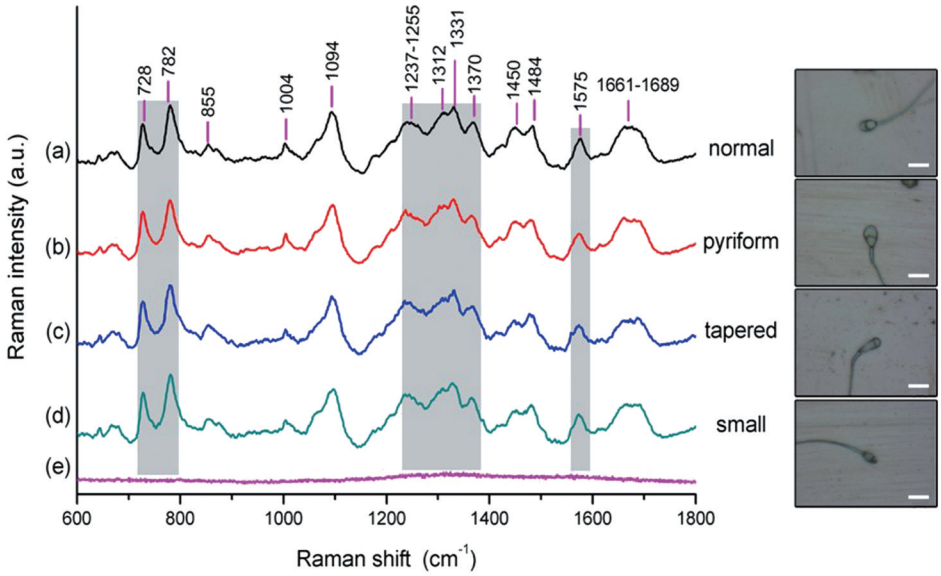

图 5 不同形貌精子的典型拉曼光谱,垂直阴影区域显示不同光谱之间的主要差异所在的光谱区域[36]

Fig. 5 Typical Raman spectra obtained from different shapes of sperms and the vertical shaded areas show the spectral regions where the main differences among different spectra are located[36]

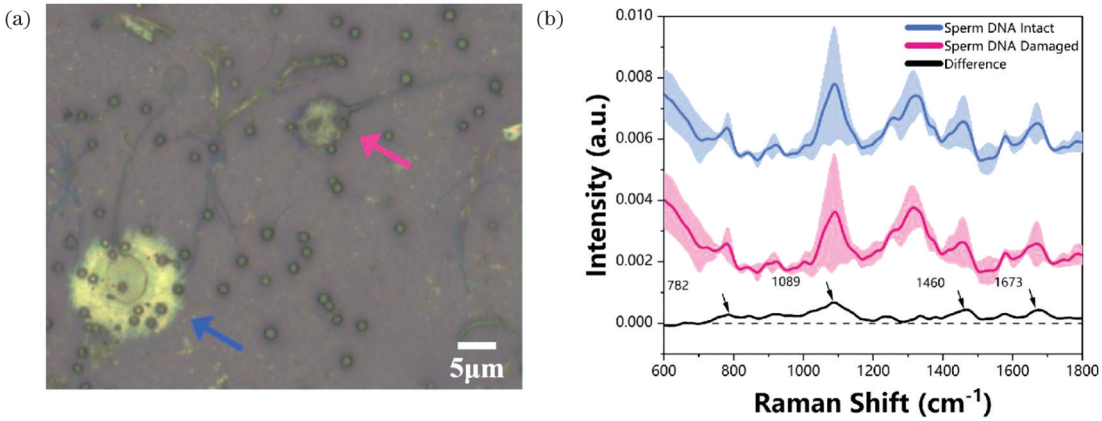

图 6 玻璃基底上染色精子细胞的明场图像以及精子细胞头部的拉曼光谱[40]。(a)染色精子的明场图像;(b)DNA 完整精子细胞(蓝线)、DNA 受损精子细胞(红色)头部的拉曼光谱以及它们的差谱(黑色)

Fig. 6 Bright-field image of stained sperms on glass substrate and Raman spectra of sperms head[40]. (a) Bright-field image of stained sperms; (b) Raman spectra obtained from DNA-intact sperm (blue line), DNA-damaged sperm (red) and their difference spectra (black)

光谱谱型存在一定的相似性和重叠性，但其特征性拉曼光谱响应差异明显。基于PCA-LDA和偏最小二乘判别分析(PLS-DA)的多元统计分析结果的对比可以发现，PLS-DA模型在精子DNA损伤组和DNA完整组间的诊断灵敏度、特异性和正确分类方面表现出相对较好的效果，如图7所示。该工作为今后进一步推动精子显微拉曼研究迈向临床应用，发展检测门槛低、兼容性好的精子评估检测提供了潜在可行性方案。

精子形态学评估侧重于反映精子的形貌质量和功能性，而拉曼光谱技术则侧重于提供精子生化质量的客观反映和无损检测评估。Huang等[41]采用疏水且表面光滑的基底实现了精子涂片的快速制备，基于该涂片无需额外的染色标记即可实现精子顶体区域的清晰识别。他们利用自编的图像分析程序实现了精子头部和顶体区域的自动分割以及形貌参数的量化，如图8(a)～(c)所示。图8(d)所示的拉曼光谱显示了精子DNA特征峰1055 cm^{-1}与1095 cm^{-1}的强度比用于评估精子DNA完整性的潜在能力。研究结果显示，显微拉曼光谱与图像分析相结合可同时提供精子的形态和生化信息，进而有望实现正常精子细胞的快速和无标记评估。

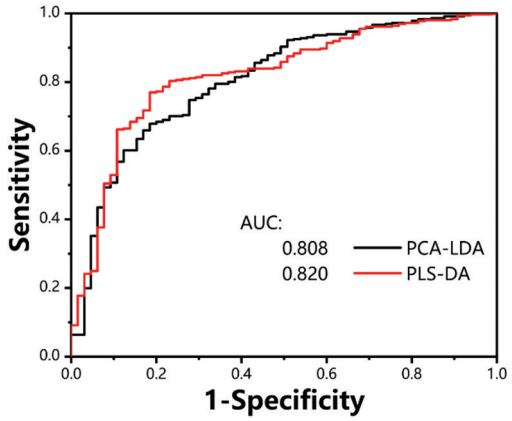

图7 完整和受损精子组的PCA-LDA和PLS-DA的受试者工作特征(ROC)曲线[40]

Fig. 7 Receiver operating characteristic (ROC) curves for PCA-LDA and PLS-DA for intact and damaged sperm groups[40]

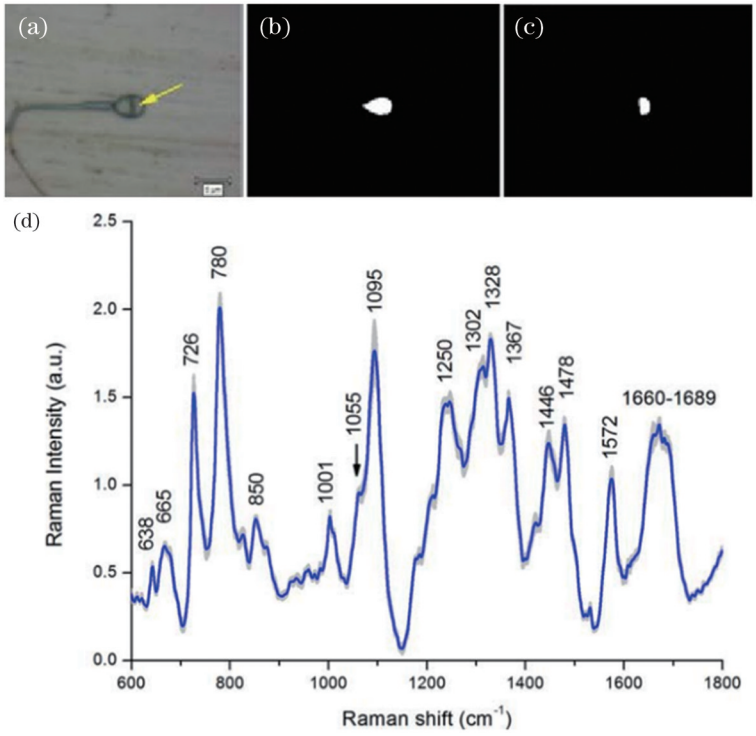

图8 精子头部及顶体区域的轮廓以及优质精子的拉曼光谱[41]。(a)精子细胞的白光图像；(b)(c)精子头部及顶体区域的轮廓；(d)优质精子在600～1800 cm^{-1}范围内的拉曼光谱

Fig. 8 Outline of sperm head and acrosome area, as well as Raman spectrum of high-quality sperm[41]. (a) A typical white light image of sperm cell; (b)(c) outline of sperm head and acrosome area; (d) Raman spectra of high-quality sperm from 600 to 1800 cm^{-1}

2016年，Ferrara等[42]首次将全息显微(HM)方法和拉曼光谱方法结合作为新型无损和非标记检测技术。图9显示了精子的全息原始图以及失焦、重建后的图形。分析不同激发功率对精子拉曼谱峰的影响后发现，30 MJ/cm^2激发功率不会对精子造成损伤。将全息显微成像与显微拉曼光谱技术结合，不仅可以凸显精子质地形貌的空间分布差异，更展示了全息显微成像与拉曼光谱分析结合的精子质量评估和鉴别的新思路。

3.2 活性精子的显微拉曼光谱研究

上述针对单精子的拉曼光谱评估虽然可以获得精子DNA状态的无损评估，但仍主要局限于固定、非生理活性或干燥条件下的精子，并非真实生理环境下活性精子的评估。辅助生殖领域中优质精

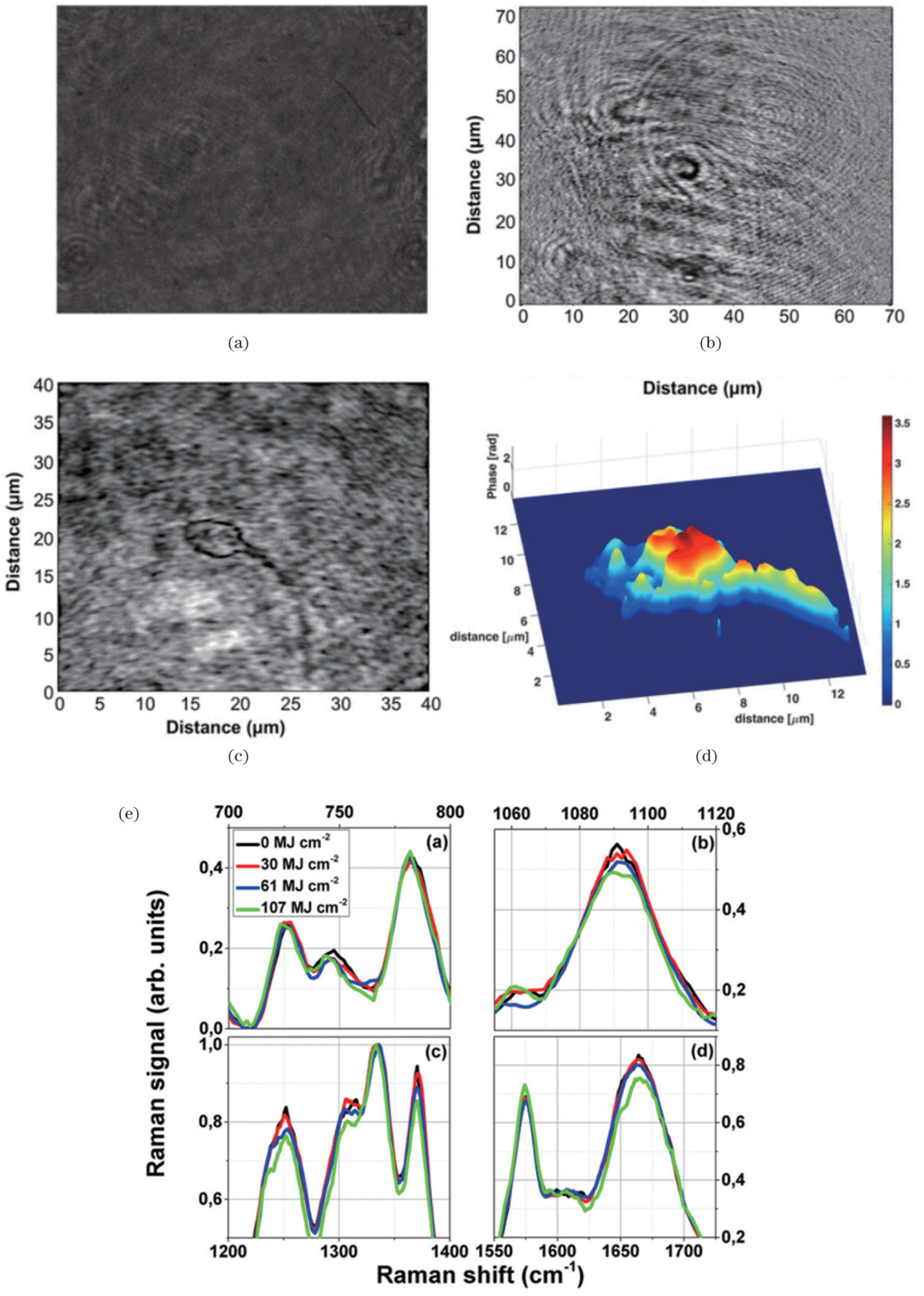

图 9 精子的全息图以及精子在不同激光功率下的光谱图[42]。(a)失焦状态下的精子细胞全息图;(b)采集平面的重建振幅图;(c)重建聚焦平面感兴趣区域的振幅图;(d)焦平面上感兴趣区域的 3D 相位图;(e)精子在 0、30、61、107 MJ/cm^{2}功率激光下不同谱峰区间的光谱图形

Fig. 9 Holographic image of sperm and its spectra of under different laser powers[42]. (a) Acquired hologram of the sperm out of focus; (b) reconstructed amplitude map at the plane of acquisition; (c) reconstructed amplitude map of the interest region at the focus plane; (d) 3D phase map of interest region at the focal plane; (e) Raman spectra acquired at laser powers of 0, 30, 61 and 107 MJ/cm^2 in various spectral regions

子的评筛不仅期望无损、非标记等评估特性，更亟须在生理环境下开展优质活性精子的评筛。实现生理环境下活性精子的“束缚”是实现稳定、可靠拉曼光谱评筛的前提和核心挑战。在受精过程中，无论是体内受精还是常规体外受精，均通过精子与卵母细胞的相互作用从生物学上选择可育精子。为此，Liu 等[43]研究了精子与卵细胞透明带（ZP）结合、透明带诱导的顶体反应以及精子不同区域的拉曼光谱强度。如图 10 所示，与透明带未结合精子的拉曼光谱相比，透明带结合精子的顶体区域（800～900 cm^{-1}和 3200～4000 cm^{-1}）光谱由低强度转变为高强度。

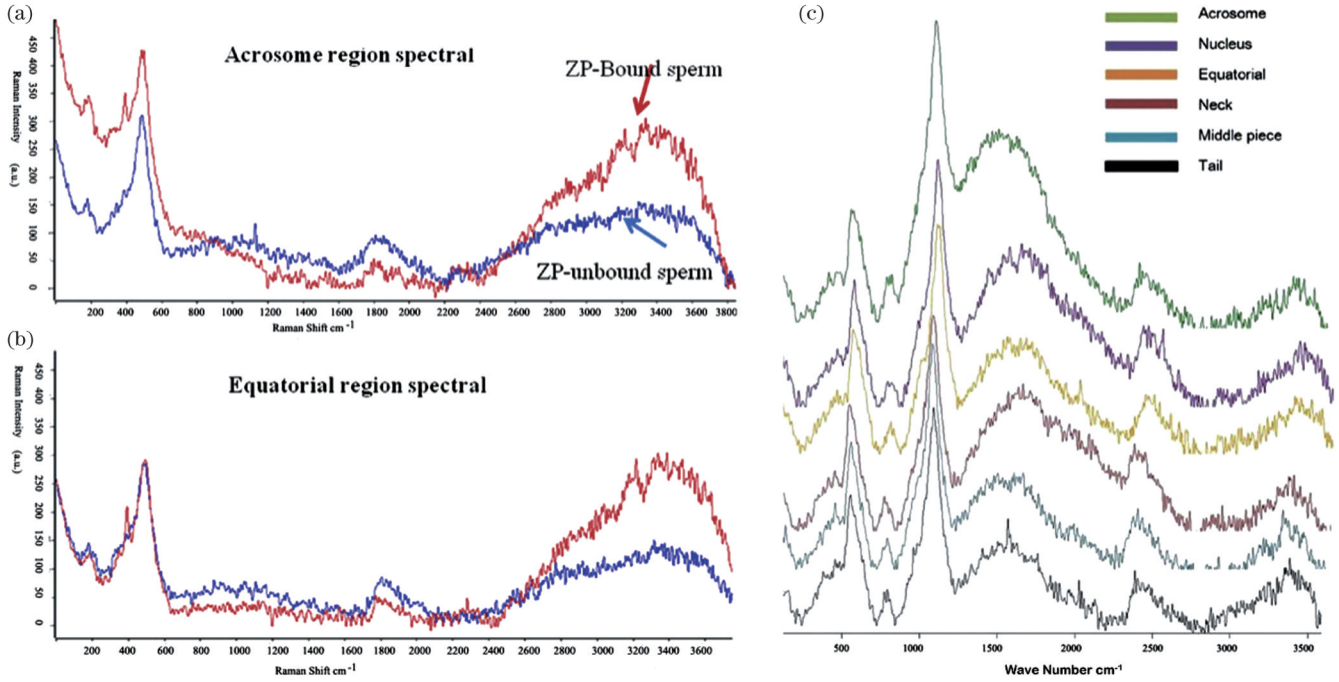

图 10 透明带结合与透明带未结合精子顶体和赤道区域的拉曼光谱对比，以及精子不同区域的光谱对比[43]。(a)透明带结合与未结合时，精子顶体区域的拉曼光谱响应（红色箭头表示与透明带结合的精子，蓝色箭头表示未与透明带结合的精子）；(b)透明带结合与未结合时，精子赤道区域的拉曼光谱响应；(c)精子不同区域的拉曼光谱对比

Fig. 10 Raman spectral comparison of acrosome and equatorial region of ZP-bound versus ZP-unbound sperm, as well as spectral comparison between various regions of the sperm[43]. (a) Raman spectral responses of sperm acrosome region for ZP-bound and ZP-unbound sperm (red arrow indicates ZP-bound sperm and blue arrow indicates ZP-unbound sperm); (b) Raman spectral responses of equatorial region for ZP-bound and ZP-unbound sperm; (c) spectral comparison between various regions of the sperm

尽管精子拉曼光谱的信噪比差，有待进一步提高，但基于主成分分析方法的统计分析表明显微拉曼光谱可以区分透明带结合精子和未结合精子。2015 年，Edengeiser 等[44]用经预处理的 CaF_2 基底“固定”吸附活动精子后，采用 60 倍水镜结合显微拉曼系统的自动测量功能，实现了在接近生理条件下单个活性精子的拉曼光谱检测，检测结果如图 11 所示。该研究工作细化了在接近生理条件下精子诱导氧化损伤的理化参数评估。

2020 年，Huang 等[45]实现了活性精子在常规基底光滑表面的固定“吸附”，然后结合水浸物镜首次获得了高信噪比的单活性精子显微拉曼光谱信号，并定性比较了活性和非活性精子的拉曼光谱差异。此外，他们还探讨了不同聚焦情形下，精子稳定束缚及拉曼信号测量效果的影响因素，如图 12 所示。

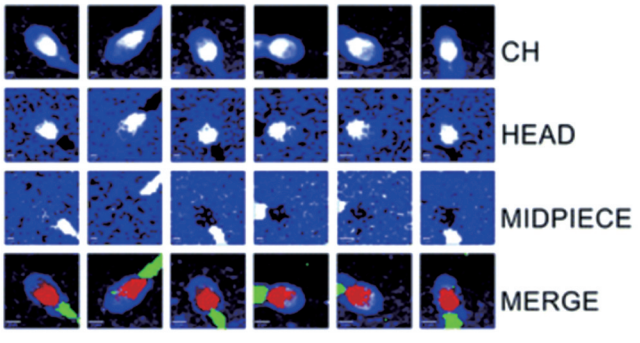

图 11 精子细胞生化成分的高光谱重建图[44]

Fig. 11 Biochemical mapping of individual living sperm reconstructed from hyperspectral datasets[44]

显然，目前基于活性精子的拉曼光谱研究尚处于初步阶段，活性精子拉曼光谱研究在实验方法和数据统计分析等方面尚有待进一步深化和完善。

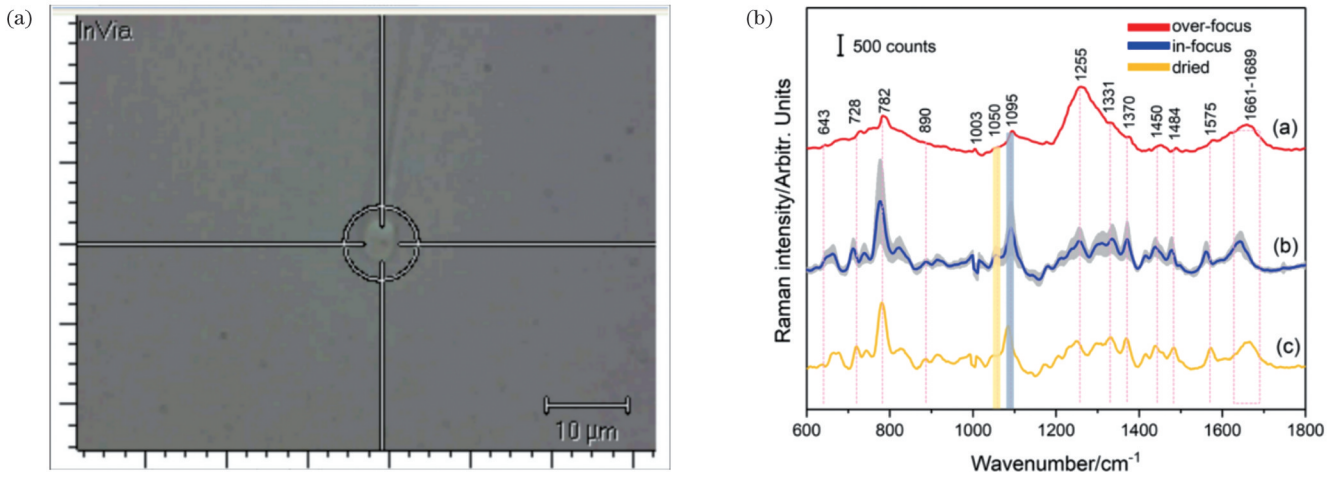

图 12 头部附着基底的活动精子的白光图及拉曼光谱图[45]。(a)白光图;(b)拉曼光谱图

Fig. 12 White light image and Raman spectra of motile sperm head attached to the substrate[45]. (a) White light image; (b) Raman spectra

4 存在的问题与发展方向

4.1 基于新型拉曼成像技术开展高时空分辨的精子刻画研究

针对非活性和生理活性精子的拉曼光谱研究展示了其在无损、客观评估精子DNA完整性方面的独特创新性和潜在优势。采用新型拉曼成像技术,如相干反斯托克斯拉曼散射(CARS)、受激拉曼散射(SRS)等,可以缩短光谱采集时间、降低荧光干扰,进而实现具有更高探测灵敏度和更精细空间分辨率的精子高速成像。因而,聚焦精子DNA损伤机制的高时空分辨研究,进而厘清精子DNA损伤程度的拉曼光谱响应以及拉曼响应的异质性,探究基于高光谱分辨与实时动态的精子生化无损评估,是后续研究进一步开展的潜在方向。此外,非活性精子的拉曼光谱检测可为活性精子拉曼光谱研究提供重要参考,因此探究非活性精子与活性精子拉曼光谱响应的关联性和差异性也是接下来研究工作的关注点。

4.2 基于微流控-显微拉曼技术的活性精子评筛

目前活性精子的显微拉曼光谱研究仍受限于精子无损"束缚"方法学的实现,缺乏简便、高效、高通量的测试评估方法。微流控技术能提供微尺度、微操纵、高通量的手段以及更接近生理状态的环境,可以最大程度地避免精子受到机械损伤和DNA过氧化损伤。构建近似于自然受精过程中精子历经不同结构、流体状态的被动式微流控通道[46-48],可以极大地缩短筛选出活力强的精子的时间。相比之下,主动式微流控技术利用主动控制所产生的外力(如电控、光控和声控)实现精子细胞的主动束缚和操纵,例如,光镊技术可以实现微流体环境下精子细胞的操纵,但光操纵的时间较长,而且高光功率密度($>10^5$ W/cm^2)潜在的光损伤不容忽视。而基于声表面波的微流控技术通过低强度声场即可实现生理活性精子细胞的无损、精确"俘获"和"操纵"[49],且长时间的声辐射场暴露并不会造成精子DNA损伤[50]。因此,将声微流控技术应用于活性精子的"俘获"和"操纵",有望实现精子的高通量、长时间、无损操作,再结合显微拉曼光谱技术,便可提供活性精子评筛的创新途径。

5 结束语

目前主流方法侧重于根据精子DNA完整性与精子形态、活动力的相关性进行优质精子的评估和筛选,缺乏直接反映活性精子DNA完整性的无损和客观评估研究。现有的精子显微拉曼检测研究仍主要局限于非生理环境下精子或非活性精子的光谱检测与刻画。将微流控技术与显微拉曼光谱技术相结合,可以实现活性精子的无损"俘获"和"操纵",进而可以实现基于显微拉曼光谱技术的活性精子DNA损伤评筛研究。以深度学习等信息技术为基础的数据综合分析与拉曼光谱技术结合将为活性精子DNA拉曼特征光谱信息的提取、DNA无损活性精子的拉曼光谱数据集构建,以及面向辅助生殖临床需求的优质精子无损评估筛选提供重要保障。多技术交叉融合有望为辅助生殖领域中DNA无损的优质精子筛选提供新方法,提高辅助生殖技术的成功率,进而促进辅助生殖领域男性不育问题研究的新发展。

参 考 文 献

[1] Perkowski J. China's one-child policy's unexpected issue[EB/OL]. [2023-01-25]. https://www.forbes.com/sites/jackperkowski/2012/05/25/chinas-one-child-policys-unexpected-issue-infertility/#3e25273e4921.

[2] Yu X J, Dong L, Ren F Q, et al. Intracytoplasmic sperm injection (ICSI) outcomes of azoospermia with different causes: 107 cases report[J]. International Journal of Clinical and Experimental Medicine, 2015, 8(11): 21684-21688.

[3] 邱峰龙, 倪蓉, 仲纪祥, 等. 不育男性不同影响因素与精子质量参数的关系研究[J]. 中国性科学, 2017, 26(5): 112-115.
Qiu F L, Ni R, Zhong J X, et al. Relationship of different influencing factors and sperm quality parameters in infertile men[J]. Chinese Journal of Human Sexuality, 2017, 26(5): 112-115.

[4] Tomlinson M J, Amissah-Arthur J B, Thompson K A, et al. Infertility: prognostic indicators for intrauterine insemination (IUI): statistical model for IUI success[J]. Human Reproduction, 1996, 11(9): 1892-1896.

[5] Pelinck M J, Hoek A, Simons A H M, et al. Efficacy of natural cycle IVF: a review of the literature[J]. Human Reproduction Update, 2002, 8(2): 129-139.

[6] Devroey P, van Steirteghem A. A review of ten years experience of ICSI[J]. Human Reproduction Update, 2004, 10(1): 19-28.

[7] Palermo G D, Neri Q V, Schlegel P N, et al. Intracytoplasmic sperm injection (ICSI) in extreme cases of male infertility[J]. PLoS One, 2014, 9(12): e113671.

[8] Zini A, Bielecki R, Phang D, et al. Correlations between two markers of sperm DNA integrity, DNA denaturation and DNA fragmentation, in fertile and infertile men[J]. Fertility and Sterility, 2001, 75(4): 674-677.

[9] Younglai E V, Holt D, Brown P, et al. Sperm swim-up techniques and DNA fragmentation[J]. Human Reproduction, 2001, 16(9): 1950-1953.

[10] Ralf H, Wolf-Bernhard S. Sperm preparation for ART[J]. Reproductive Biology and Endocrinology, 2003, 1(1): 108.

[11] Muratori M, Tarozzi N, Carpentiero F, et al. Sperm selection with density gradient centrifugation and swim up: effect on DNA fragmentation in viable spermatozoa[J]. Scientific Reports, 2019, 9(1): 1-12.

[12] Hansen M, Bower C, Milne E, et al. Assisted reproductive technologies and the risk of birth defects: a systematic review[J]. Human Reproduction, 2005, 20(2): 328-338.

[13] Aitken R J, De Iuliis G N. Origins and consequences of DNA damage in male germ cells[J]. Reproductive BioMedicine Online, 2007, 14(6): 727-733.

[14] Aitken R J, De Iuliis G N. On the possible origins of DNA damage in human spermatozoa[J]. Molecular Human Reproduction, 2010, 16(1): 3-13.

[15] Muriel L, Goyanes V, Segrelles E, et al. Increased aneuploidy rate in sperm with fragmented DNA as determined by the sperm chromatin dispersion (SCD) test and FISH analysis[J]. Journal of Andrology, 2007, 28(1): 38-49.

[16] Evenson D, Jost L. Sperm chromatin structure assay is useful for fertility assessment[J]. Methods in Cell Science, 2000, 22(2): 169-189.

[17] Singh N P, McCoy M T, Tice R R, et al. A simple technique for quantitation of low levels of DNA damage in individual cells[J]. Experimental Cell Research, 1988, 175(1): 184-191.

[18] Olive P L, Banáth J P. The comet assay: a method to measure DNA damage in individual cells[J]. Nature Protocols, 2006, 1(1): 23-29.

[19] Diem M. Modern vibrational spectroscopy and micro-spectroscopy: theory, instrumentation, and biomedical applications[M]. Singapore: John Wiley & Sons, 2015.

[20] Fournier F, Guo R, Gardner E M, et al. Biological and biomedical applications of two-dimensional vibrational spectroscopy: proteomics, imaging, and structural analysis[J]. Accounts of Chemical Research, 2009, 42(9): 1322-1331.

[21] Huang Z W, McWilliams A, Lui H, et al. Near-infrared Raman spectroscopy for optical diagnosis of lung cancer[J]. International Journal of Cancer, 2003, 107(6): 1047-1052.

[22] Chan J W, Taylor D S, Zwerdling T, et al. Micro-Raman spectroscopy detects individual neoplastic and normal hematopoietic cells[J]. Biophysical Journal, 2006, 90(2): 648-656.

[23] Berger A J, Itzkan I, Feld M S. Feasibility of measuring blood glucose concentration by near-infrared Raman spectroscopy[J]. Spectrochimica Acta Part A: Molecular and Biomolecular Spectroscopy, 1997, 53(2): 287-292.

[24] Neto L P M, Silva L F D C E, Dos Santos L, et al. Micro-Raman spectroscopic study of thyroid tissues[J]. Photodiagnosis and Photodynamic Therapy, 2017, 17: 164-172.

[25] Sugimura T, Kajimoto S, Nakabayashi T. Label-free imaging of intracellular temperature by using the O — H stretching Raman band of water[J]. Angewandte Chemie International Edition, 2020, 59(20): 7755-7760.

[26] 路交, 朱姗姗, 崔笑宇, 等. 拉曼光谱成像技术及其在生物医学中的应用[J]. 中国激光, 2018, 45(3): 0307007.
Lu J, Zhu S S, Cui X Y, et al. Raman spectroscopic imaging technology and its biomedical applications[J]. Chinese Journal of Lasers, 2018, 45(3): 0307007.

[27] 刘风翔, 张礼豪, 黄霞. 拉曼光谱技术在肿瘤诊断中的应用[J]. 激光与光电子学进展, 2022, 59(6): 0617016.
Liu F X, Zhang L H, Huang X. Application of Raman spectroscopy in cancer diagnosis[J]. Laser & Optoelectronics Progress, 2022, 59(6): 0617016.

[28] Enejder A M K, Koo T W, Oh J, et al. Blood analysis by Raman spectroscopy[J]. Optics Letters, 2002, 27(22): 2004-2006.

[29] Premasiri W R, Clarke R H, Womble M E. Urine analysis by laser Raman spectroscopy[J]. Lasers in Surgery and Medicine, 2001, 28(4): 330-334.

[30] Wang H, Malvadkar N, Koytek S, et al. Quantitative analysis of creatinine in urine by metalized nanostructured parylene[J]. Journal of Biomedical Optics, 2010, 15(2): 027004.

[31] Gonchukov S, Sukhinina A, Bakhmutov D, et al. Raman spectroscopy of saliva as a perspective method for periodontitis diagnostics[J]. Laser Physics Letters, 2012, 9(1): 73-77.

[32] Itzkan I, Qiu L, Fang H, et al. Confocal light absorption and scattering spectroscopic microscopy monitors organelles in live cells with no exogenous labels[J]. Proceedings of the National Academy of Sciences of the United States of America, 2007, 104(44): 17255-17260.

[33] Gianaroli L, Magli M C, Ferraretti A P, et al. Birefringence characteristics in sperm heads allow for the selection of reacted spermatozoa for intracytoplasmic sperm injection[J]. Fertility and Sterility, 2010, 93(3): 807-813.

[34] Huser T, Orme C A, Hollars C W, et al. Raman spectroscopy of DNA packaging in individual human sperm cells distinguishes normal from abnormal cells[J]. Journal of Biophotonics, 2009, 2(5): 322-332.

[35] Meister K, Schmidt D A, Bründermann E, et al. Confocal Raman microspectroscopy as an analytical tool to assess the mitochondrial status in human spermatozoa[J]. The Analyst, 2010, 135(6): 1370-1374.

[36] Mallidis C, Wistuba J, Bleisteiner B, et al. *In situ* visualization of damaged DNA in human sperm by Raman microspectroscopy[J]. Human Reproduction, 2011, 26(7): 1641-1649.

[37] da Costa R, Amaral S, Redmann K, et al. Spectral features of nuclear DNA in human sperm assessed by Raman microspectroscopy: effects of UV-irradiation and hydration[J]. PLoS One, 2018, 13(11): e0207786.

[38] Sánchez V, Redmann K, Wistuba J, et al. Oxidative DNA damage in human sperm can be detected by Raman microspectroscopy[J]. Fertility and Sterility, 2012, 98(5): 1124-1129.

[39] Huang Z F, Chen X, Chen G N, et al. Characterization and differentiation of normal and abnormal spermatozoa via micro-Raman spectroscopy[J]. Laser Physics Letters, 2013, 10(3): 035601.

[40] Du S R, Zhang Q, Guan H H, et al. Micro-Raman analysis of sperm cells on glass slide: potential label-free assessment of sperm DNA toward clinical applications[J]. Biosensors, 2022, 12(11): 1051.

[41] Huang Z F, Chen G N, Chen X W, et al. Rapid and label-free identification of normal spermatozoa based on image analysis and micro-Raman spectroscopy[J]. Journal of Biophotonics, 2014, 7(9): 671-675.

[42] Ferrara M A, de Angelis A, de Luca A C, et al. Simultaneous holographic microscopy and Raman spectroscopy monitoring of human spermatozoa photodegradation[J]. IEEE Journal of Selected

Topics in Quantum Electronics, 2016, 22(3): 27-34.
[43] Liu F, Zhu Y, Liu Y F, et al. Real-time Raman microspectroscopy scanning of the single live sperm bound to human zona pellucida[J]. Fertility and Sterility, 2013, 99(3): 684-689.
[44] Edengeiser E, Meister K, Bründermann E, et al. Non-invasive chemical assessment of living human spermatozoa[J]. RSC Advances, 2015, 5(14): 10424-10429.
[45] Huang Z F, Du S R, Liang X Z, et al. Head-attached live sperm cell for label-free micro-Raman evaluation of sperm DNA integrity: a preliminary study[J]. Journal of Raman Spectroscopy, 2020, 51(4): 591-595.
[46] Simchi M, Riordon J, You J B, et al. Selection of high-quality sperm with thousands of parallel channels[J]. Lab on a Chip, 2021, 21(12): 2464-2475.
[47] Vasilescu S A, Khorsandi S, Ding L, et al. A microfluidic approach to rapid sperm recovery from heterogeneous cell suspensions[J]. Scientific Reports, 2021, 11(1): 1-11.
[48] Xiao S, Riordon J, Simchi M, et al. FertDish: microfluidic sperm selection-in-a-dish for intracytoplasmic sperm injection[J]. Lab on a Chip, 2021, 21(4): 775-783.
[49] Gai J Y, Nosrati R, Neild A. High DNA integrity sperm selection using surface acoustic waves[J]. Lab on a Chip, 2020, 20(22): 4262-4272.
[50] Ozcelik A, Rufo J, Guo F, et al. Acoustic tweezers for the life sciences[J]. Nature Methods, 2018, 15(12): 1021-1028.

Recent Progress in Sperm Evaluation and Screening Based on Raman Spectroscopy

Huang Zufang[1*], Li Yuling[1], Du Shengrong[2], Sun Yan[2], Wang Jiarui[1], Zhang Qun[1], Chen Rong[1]

[1]*College of Photonic and Electronic Engineering, Key Laboratory of Opto-Electronic Science and Technology for Medicine of Ministry of Education, Fujian Provincial Key Laboratory for Photonics Technology, Fujian Normal University, Fuzhou* 350117, *Fujian, China*;

[2]*Reproductive Center, Fujian Maternity and Child Health Hospital, Fuzhou* 350001, *Fujian, China*

Abstract

Significance The quality of sperm in fertile men worldwide is deteriorating. Although sperm quality is not directly related to male infertility, it is strongly linked to subfertility. Assisted reproductive technology addresses common male infertility issues, such as low sperm count, abnormal morphology, and motility, and it is the primary technological solution to male infertility through the evaluation and screening of high-quality sperm. However, current clinical research is limited to screening sperm morphology and motility, and there is a lack of non-destructive screening methods for evaluating sperm DNA damage. This review article first introduces the demand for non-destructive sperm screening technology in assisted reproduction and the basic principle of micro-Raman spectroscopy, and then summarizes current Raman-based research progress on sperm. Next, a comprehensive analysis and discussion of Raman detection and Raman spectral characteristics of sperm cells are conducted, emphasizing the Raman response to sperm DNA damage. Finally, the potential for applied research in non-destructive sperm evaluation and screening is discussed and explored.

Progress Raman-based sperm analysis is still in the initial stage of development, but the unique advantages of Raman spectroscopy have opened up new routes for sperm characterization. In 2009, Huser *et al*. used micro-Raman spectroscopy to correlate the spectral response of chromatin differences with sperm morphology. Meister *et al*. achieved Raman imaging characterization of sperm nucleus, neck, and mitochondria in sperm cells. By simulating the damaging effect of UV radiation on different sperm organelles, it was verified that micro-Raman spectroscopy is expected to provide a new method for rapid assessment of sperm mitochondrial status. Subsequently, Mallidis *et al*. reported that the damage to sperm DNA due to UV radiation is mainly reflected in the intensity change of the PO_4 skeleton peak (1042 cm^{-1}) attributed to DNA. Additionally, the spectral response of sperm DNA damage due to UV light was only observed in dry conditions, not in solution media. A comparison of Raman results of sperm DNA and flow cytometry revealed different responses of sperm DNA damage to the characteristic peak intensities. Given the challenges of labor-intensive sperm sample processing in earlier research and the potential impact on Raman test outcomes, Huang *et al*. collected microscopic Raman spectrum data of normal and various abnormal morphology (pear-shaped, cone-shaped, small-headed) based on a new Raman test substrate. They achieved rapid sample preparation (tens of seconds) and effective classification using principal component analysis and linear discriminant methods (PCA-LDA) on the new substrates. Additionally, combined with the extended multiplicative signal correction (EMSC) method, Raman detection of DNA-intact and DNA-damaged sperm cells on glass slides was attempted, effectively "filtering" glass signal interference and obtaining the intrinsic Raman signal of sperm. Huang *et al*. also achieved rapid preparation of sperm samples, automatic segmentation of sperm head and acrosome regions, and quantification of morphology parameters using a hydrophobic substrate and image analysis. In 2016, Ferrara *et al*. combined holographic microscopic imaging with microscopic Raman spectroscopy not only to highlight the differences in sperm quality and morphology's spatial distribution but also to show a novel method for sperm quality assessment in conjunction with sperm morphology assessment and Raman spectroscopy analysis.

Regarding the Raman assessment of motile sperm, in 2012, Feng Liu *et al*. studied the interaction of sperm and the zona pellucida (ZP), the acrosome reaction induced by the zona pellucida, and the Raman spectral response of different regions of sperm.

Hence, the acrosome region (800–900 and 3200–4000 cm^{-1}) of zona-bound sperm shifted from mild hypointensity to hyperintensity compared to the Raman spectra of zona-bound sperm. In 2015, Edengeiser *et al*. achieved the "fixed" adsorption of motile sperm on the pretreated CaF_2 substrate. Combined with the automatic measurement in the micro-Raman system, they detected a single motile sperm under physiological conditions. Raman spectroscopic detection allows the assessment of physicochemical parameters of sperm-induced oxidative damage under near-physiological conditions. Conversely, in 2020, Huang *et al*. realized the fixed "adsorption" of motile sperm on the smooth surface of a conventional substrate. For the first time, they obtained a Raman spectrum with a high signal-to-noise ratio from a single motile sperm using a water immersion objective and qualitatively compared motile and non-motile sperm. Additionally, the influencing factors of the stable "fixation" of sperm and Raman signal under different focusing conditions were discussed. Raman-based motile sperm study is still in its early stages, requiring more development and improvement in terms of experimental techniques and statistical data processing.

Conclusions and Prospects Traditionally, high-quality sperm evaluation and screening have focused on the relationship between sperm DNA integrity and sperm morphology and motility. However, a lack of non-destructive and objective evaluation research directly reflects the integrity of active sperm DNA. The current research on sperm microscopic Raman detection is still in its early stages and is mainly limited to detecting and characterizing spermatozoa or immotile sperm in non-physiological environments. The combination of microfluidic devices and micro-Raman spectroscopy can achieve non-destructive "capture" and "manipulation" of motile sperm. Based on this, research on DNA damage assessment of motile sperm using micro-Raman spectroscopy is being conducted. The integration of data comprehensive analysis based on information technology, such as deep learning and Raman spectroscopy technology, can effectively extract the Raman spectral information of motile sperm DNA, establish the Raman spectral dataset of motile sperm with intact DNA, and thus provide high-quality data for clinical assisted reproduction needs. The multi-technology integration is expected to provide an objective and non-destructive new method for DNA-intact high-quality sperm screening in the field of assisted reproduction, improve the success rate of male-factor assisted reproductive technology, and promote new developments and opportunities in the study of male infertility in the field of assisted reproduction.

Key words medical optics; Raman spectroscopy; sperm; DNA damage; evaluation and screening; statistical analysis